Joint Radar Waveform and Bank of Filter Design for Wind Farm Clutter Mitigation

Domenico Gaglione*, Augusto Aubry†, Carmine Clemente‡
Antonio De Maio†, John J. Soraghan‡ and Alfonso Farina§

***Abstract*—In-shore and off-shore wind farms are nowadays representing strategic assets for the generation of clean energy. However their presence interferes with existing surveillance systems, such as primary radar systems. In order to achieve painless coexistence of radar and wind farms systems, solutions can be explored from both the renewable energy and radar communities. In particular, this paper deals with the latter aspect, proposing signal processing solutions able to allow a radar system to mitigate the deleterious effects of a wind farm within its surveillance area. This paper proposes a joint radar waveform and filter design aimed to optimize the Signal plus Interference to Noise Power Ratio (SINR) in a multi-static radar scenario. The analysis is performed on simulated data and shows that the proposed method is able to reduce the effect of wind farms.**

Keywords*—*Wind farms, optimization, SINR, multi-static radars, primary radars.

I. Introduction

The capability of radar systems to adapt to the changing surrounding environment has become an important requirement in the modern radar sensing scenarios. More often, political and economical factors introduce novel elements on the radar chessboard that can affect the effectiveness of the radar to accomplish its tasks. The human intervention is often changing the characteristics of the radar scenario, adding electromagnetic interferers (novel communication infrastructure) and non-stationary clutter sources (wind farms). In particular, the presence of wind farms within the surveillance area of a radar system affects dramatically the target detection capabilities [1]. The large radar cross-section of wind turbines in conjunction with the time-varying Doppler modulation injected on the radar returns decreases the capability of a radar to detect moving targets, such as aircraft flying over a land or an off-shore wind farm.

The effects of the wind farms on radar systems have been widely modeled and studied, including those on more advanced radar modes [1]–[3]. The electromagnetic interference (EMI) of wind turbines in polarimetric radar systems has been studied in [1], identifying some discriminating features that can be used in order to distinguish wind turbines from actual targets. In [2] the effect of the wind turbines on Synthetic Aperture Radar (SAR) images has been modeled and potential issues on the final product quality and target detection have been discussed. The use of spatial and frequency diversities is suggested in [3] with an analysis on the radar returns from S and X band radar data in mono and bistatic configurations.

Signal processing based solutions to the problem of EMI from wind turbines have been investigated in the literature [4]–[6]. In [4] waveform design within a Coherent Pulse integration Interval (CPI) is proposed to resolve ambiguous ranges and filter out wind turbines' returns. The proposed solution resides in randomizing parameters in the transmitted train of pulses in order to design filters able to reject both clutter and echoes from wind turbines. A seasonal moving average filter is used in [5] in order to exploit the cyclostationary properties of the wind turbine returns to filter out the undesired echoes for the specific case of weather radar applications. This approach showed good capabilities achieving up to 20 dBs of wind turbine clutter rejection. The specific case of wind turbines clutter mitigation in Air Traffic Control radars is addressed in [6], with a solution based on the GAPES (Gapped-data Amplitude and Phase Estimation) algorithm to fill gaps in data measurements and the computation of a correction function from time-frequency distributions in order to remove the wind turbines' effect.

In this paper we propose a novel strategy for the joint design of radar waveform and bank of filters in order to maximize the detection probability in a distributed radar network. In particular, we extend the approach proposed in [7] to obtain the optimal design to mitigate the effect of a wind farm on a multi-static radar system. The basic idea of the proposed approach is to optimize the worst case SINR by reformulating the original non-convex max-min optimization problem. The proposed algorithm is an optimization procedure that monotonically improves the worst-case SINR. A convex and a generalized fractional programming problem are involved in each iteration; the latter is solved through the Dinkelbach's procedure with polynomial complexity. The remainder of the paper is organized as follows. Section II derives the signal model for the analyzed multi-static radar scenario. Section III formulates the optimization problem and the optimization procedure. Results on simulated data are discussed in Section IV while Section V concludes the paper.

II. Signal Model

A multi-static radar system with one transmitter and Q receivers is considered, which operates in proximity of a wind

*NATO STO Centre for Maritime Research and Experimentation, La Spezia, Italy (domenico.gaglione@cmre.nato.int).

†Università degli Studi di Napoli "Federico II", DIETI, via Claudio 21, I-80125 Napoli, Italy (augusto.aubry@unina.it, ademaio@unina.it).

‡University of Strathclyde, CESIP, EEE, 204, George Street, G1 1XW, Glasgow, UK (carmine.clemente@strath.ac.uk, j.soraghan@strath.ac.uk).

§FIET, LFIEEE, Selex-ES (retired), Visiting Professor UCL, Rome, Italy (alfonso.farina@outlook.it).

Domenico Gaglione and John Soraghan's work was supported by the Engineering and Physical Sciences Research Council (EPSRC) Grant number EP/K014307/1 and the MOD University Defence Research Collaboration in Signal Processing.

978-1-5386-1663-5/17 /$31.00 ©2017 IEEE

farm. The system, and in particular the receivers, are designed to process the signal received from each multi-static radar cell, and then send the result to a fusion centre for target detection. The K radar cells, of dimensions driven by the resolution of the system itself, are defined through an absolute reference system, that is not linked to any transmitter-receiver pair. Moreover, both the K cells that form the surveillance volume, and the wind farm, are assumed to be within the unambiguous range of the system[1]. Let[2] $\boldsymbol{s} = [s(1), s(2), \cdots, s(N)]^T \in \mathbb{C}^N$ denote the slow-time code used by the transmitter to form a coherent burst of N slow-time coded pulses, and $\boldsymbol{v}^{(q,k)} \in \mathbb{C}^N$ be the vector containing the observations from the k-th radar cell at the q-th receiver, with $k = 1, \ldots, K$ and $q = 1, \ldots, Q$. Furthermore, let us define the generic steering vector $\boldsymbol{p}(x)$ as:

$$\boldsymbol{p}(x) = \left[1, e^{-j2\pi x}, \ldots, e^{-j2\pi(N-1)x}\right]^T \in \mathbb{C}^N \tag{1}$$

Then, the vector $\boldsymbol{v}^{(q,k)}$ can be expressed as:

$$\boldsymbol{v}^{(q,k)} = \boldsymbol{t}^{(q,k)} + \boldsymbol{d}^{(q,k)} + \boldsymbol{n}^{(q)} \tag{2}$$

where each of the three contributions is a circular symmetric random vector. Description and statistical characterisation of $\boldsymbol{t}^{(q,k)}$, $\boldsymbol{d}^{(q,k)}$ and $\boldsymbol{n}^{(q)}$ are reported below.

The vector $\boldsymbol{t}^{(q,k)}$ represents the return from the target, equal to:

$$\boldsymbol{t}^{(q,k)} = \alpha^{(q,k)} \left(\boldsymbol{s} \odot \boldsymbol{p}\left(\mu^{(q)}\right)\right) \tag{3}$$

where $\mu^{(q)} = T_s f_t^{(q)}$ is the unknown normalised target's Doppler frequency, with T_s and $f_t^{(q)}$ the Pulse Repetition Interval (PRI) and the actual target Doppler frequency, respectively, while $\mathrm{var}\left(\alpha^{(q,k)}\right) = \mathbb{E}\left[\left|\alpha^{(q,k)}\right|^2\right]$ is the power of the return, that accounts for channel propagation and scattering effects from the target.

The vector $\boldsymbol{d}^{(q,k)}$ contains the filtered signal-dependent interfering samples, due to clutter (returns from land, rain, etc.) and to the rotation of the wind turbine's blades, which is located in the k-th radar cell[3]. It is expressed as:

$$\begin{aligned}\boldsymbol{d}^{(q,k)} = &\sum_{l=0}^{L-1}\sum_{m=0}^{M-1} \beta_{m,l}^{(q,k)} \left(\boldsymbol{s} \odot \boldsymbol{p}\left(\nu_{m,l}^{(q,k)}\right)\right) \\ &+ \sum_{k'=0}^{N_C} \gamma_{k'}^{(q,k)} \boldsymbol{J}_{k'} \left(\boldsymbol{s} \odot \boldsymbol{p}\left(\xi_{k'}^{(q,k)}\right)\right)\end{aligned} \tag{4}$$

As to the wind turbine contribution, M is the number of uncorrelated point scatterers located on each of the L blades of the wind turbine, and $\mathrm{var}\left(\beta_{m,l}^{(q,k)}\right) = \mathbb{E}\left[\left|\beta_{m,l}^{(q,k)}\right|^2\right]$ and $\nu_{m,l}^{(q,k)}$ are the power and the normalised Doppler frequency of the return from the (m,l)-th point scatterer, with the latter being uniformly distributed in the range $\left[\overline{\nu}_{m,l}^{(q,k)} - \delta_{m,l}^{(q,k)}, \overline{\nu}_{m,l}^{(q,k)} + \delta_{m,l}^{(q,k)}\right]$[4]. Such a geometric formulation of the return signal from the wind turbine's blades, despite being simplified, reasonably models the dynamic of the problem. Moreover, possible mismatches, due to, for example, vibrations of the mast, are taken into account in the definition of the random interval of the normalised Doppler frequency $\nu_{m,l}^{(q,k)}$. Regarding the signal-dependent interference contribution, $N_C \leq N-1$ is the number of ambiguous range cells that interfere with the one of interest. Moreover, $\mathrm{var}\left(\gamma_{k'}^{(q,k)}\right) = \mathbb{E}\left[\left|\gamma_{k'}^{(q,k)}\right|^2\right]$ and $\xi_{k'}^{(q,k)}$ are the power and the normalised Doppler frequency of the clutter, respectively, with the latter uniformly distributed in $\left[\overline{\xi}_{k'}^{(q,k)} - \varepsilon_{k'}^{(q,k)}, \overline{\xi}_{k'}^{(q,k)} + \varepsilon_{k'}^{(q,k)}\right]$, while $\boldsymbol{J}_{k'}$ is the shift matrix defined as:

$$\boldsymbol{J}_{k'}(x, x') = \begin{cases} 1 & x - x' = k' \\ 0 & x - x' \neq k' \end{cases} \tag{5}$$

The covariance matrix of $\boldsymbol{d}$ is equal to:

$$\begin{aligned}\boldsymbol{\Gamma}_{\boldsymbol{d}}^{(q,k)}(\boldsymbol{s}) &= \mathbb{E}\left[\boldsymbol{d}^{(q,k)} \boldsymbol{d}^{(q,k)\dagger}\right] = \\ &= \sum_{l=0}^{L-1}\sum_{m=0}^{M-1} \mathrm{var}\left(\beta_{m,l}^{(q,k)}\right) \boldsymbol{S}\, \boldsymbol{\Psi}_{m,l}^{(q,k)} \boldsymbol{S}^\dagger \\ &+ \sum_{k'=0}^{N_C} \mathrm{var}\left(\gamma_{k'}^{(q,k)}\right) \boldsymbol{J}_{k'} \boldsymbol{S}\, \boldsymbol{\Phi}_{k'}^{(q,k)} \boldsymbol{S}^\dagger \boldsymbol{J}_{k'}^T\end{aligned} \tag{6}$$

[1] This assumption will be relaxed in future developments.

[2] We adopt the notation of using boldface for column vectors $\boldsymbol{a}$ (lower case), and matrices $\boldsymbol{A}$ (upper case). The transpose, the conjugate, and the conjugate transpose operators are denoted by the symbols $(\cdot)^T$, $(\cdot)^*$ and $(\cdot)^\dagger$ respectively. $\mathrm{diag}(\boldsymbol{a})$ indicates the diagonal matrix whose i-th diagonal element is the i-th entry of $\boldsymbol{a}$. $\boldsymbol{I}$ and $\boldsymbol{0}$ denote respectively the identity matrix and the matrix with zero entries (their size is determined from the context). $\mathbb{C}^N$ and $\mathbb{H}^N$ are respectively the sets of N-dimensional vectors of complex numbers and $N \times N$ Hermitian matrices. The curled inequality symbol $\succeq$ (and its strict form $\succ$) is used to denote generalized matrix inequality: for any $\boldsymbol{A} \in \mathbb{H}^N$, $\boldsymbol{A} \succeq \boldsymbol{0}$ means that $\boldsymbol{A}$ is a positive semidefinite matrix ($\boldsymbol{A} \succ \boldsymbol{0}$ for positive definiteness). The Euclidean norm of the vector $\boldsymbol{x}$ is denoted by $\|\boldsymbol{x}\|$. The letter j represents the imaginary unit (i.e. $j = \sqrt{-1}$), while the letter i often serves as index in this paper. For any complex number x, we use $\Re(x)$, $|x|$, and $\arg(x)$ to denote respectively the real part, the modulus, and the argument of x. $\mathbb{E}[\cdot]$ denotes the statistical expectation. Finally, $\odot$ denotes the Hadamard product and for any optimization problem $\mathcal{P}$, $v(\mathcal{P})$ represents its optimal value.

[3] Without loss of generality, it is supposed that at most one wind turbine is located in the k-th radar cell. Moreover, assuming low range side lobes of the employed waveform, the interference from neighbouring radar cells is considered negligible.

[4] The expression of $\overline{\nu}_{m,l}^{(q,k)}$, not reported in this paper for conciseness and left for a later publication, depends on the structure of the wind turbine (number and relative dimension of the blades w.r.t. the wavelength of the radar), its rotation speed and its orientation w.r.t to both the transmitter and the q-th receiver.

where $\boldsymbol{S} = \mathrm{diag}\{\boldsymbol{s}\}$,

$$\boldsymbol{\Psi}_{m,l}^{(q,k)}(x,x') = \\ = \begin{cases} 1 & x = x' \\ e^{-j2\pi\overline{\nu}_{m,l}^{(q,k)}(x-x')} \frac{\sin\left[2\pi\delta_{m,l}^{(q,k)}(x-x')\right]}{2\pi\,\delta_{m,l}^{(q,k)}(x-x')} & x \neq x' \end{cases} \quad (7)$$

and

$$\boldsymbol{\Phi}_{k'}^{(q,k)}(x,x') = \\ = \begin{cases} 1 & x = x' \\ e^{-j2\pi\overline{\xi}_{k'}^{(q,k)}(x-x')} \frac{\sin\left[2\pi\varepsilon_{k'}^{(q,k)}(x-x')\right]}{2\pi\,\varepsilon_{k'}^{(q,k)}(x-x')} & x \neq x' \end{cases} \quad (8)$$

The vector $\boldsymbol{n}^{(q)}$ represents the filtered signal-independent coloured noise, with $\boldsymbol{\Gamma}_{\boldsymbol{n}}^{(q)} = \mathbb{E}\left[\boldsymbol{n}^{(q)}\boldsymbol{n}^{(q)^\dagger}\right] \succ \boldsymbol{0}$ so as to account for both white internal noise and other signal-independent interferences. In the next section the optimization problem in this scenario will be formulated.

III. Problem Formulation and Design Issues

The joint design of the radar code and the receive architecture optimizing the worst-case SINR over the unknown target state is addressed forcing some practical constraints on the shape of the transmit code. Specifically, the slow-time received signals from a specific radar cell k, that is $\boldsymbol{v}^{(q,k)}$ for $q = 1,\ldots,Q$, are processed through a specific bank of filters

$$\boldsymbol{w}_{k,i} = \left[\boldsymbol{w}_{k,i}^{(1)^\dagger},\ldots,\boldsymbol{w}_{k,i}^{(Q)^\dagger}\right]^\dagger \quad (9)$$

where $\boldsymbol{w}_{k,i}^{(q)} \in \mathbb{C}^N$, $i \in \mathcal{A}_k$, and $\mathcal{A}_k$ is the set of velocity bins of interest for the k-th cell, where each velocity bin corresponds to a specific pull of Q values, $\left\{\mu_i^{(1)},\ldots,\mu_i^{(Q)}\right\}$. The SINR at the k-th radar cell on the i-th branch can be written as:

$$\mathrm{SINR}_{k,i} = \frac{\sum_{q=1}^{Q} \mathrm{var}\left(\alpha^{(q,k)}\right)\left|\left(\boldsymbol{s}\odot\boldsymbol{p}\left(\mu_i^{(q)}\right)\right)^\dagger \boldsymbol{w}_{k,i}^{(q)}\right|^2}{\boldsymbol{w}_{k,i}^\dagger\boldsymbol{\Sigma}_{\boldsymbol{d}}^{(k)}(\boldsymbol{s})\,\boldsymbol{w}_{k,i} + \boldsymbol{w}_{k,i}^\dagger\boldsymbol{\Sigma}_{\boldsymbol{n}}\,\boldsymbol{w}_{k,i}} \quad (10)$$

where $\boldsymbol{\Sigma}_{\boldsymbol{d}}^{(k)}(\boldsymbol{s})$ and $\boldsymbol{\Sigma}_{\boldsymbol{n}}$ are block diagonal matrices defined as follows:

$$\boldsymbol{\Sigma}_{\boldsymbol{d}}^{(k)}(\boldsymbol{s}) = \mathrm{diag}\left\{\boldsymbol{\Gamma}_{\boldsymbol{d}}^{(1,k)}(\boldsymbol{s}),\ldots,\boldsymbol{\Gamma}_{\boldsymbol{d}}^{(Q,k)}(\boldsymbol{s})\right\} \quad (11)$$

$$\boldsymbol{\Sigma}_{\boldsymbol{n}} = \mathrm{diag}\left\{\boldsymbol{\Gamma}_{\boldsymbol{n}}^{(1)},\ldots,\boldsymbol{\Gamma}_{\boldsymbol{n}}^{(Q)}\right\} \quad (12)$$

The numerator of (10) is the useful average energy at the output of the i-th filter associated to the k-th radar cell of the overall multi-static radar, while $\boldsymbol{w}_{k,i}^\dagger\boldsymbol{\Sigma}_{\boldsymbol{d}}^{(k)}(\boldsymbol{s})\,\boldsymbol{w}_{k,i}$ and $\boldsymbol{w}_{k,i}^\dagger\boldsymbol{\Sigma}_{\boldsymbol{n}}\,\boldsymbol{w}_{k,i}$ represent the clutter plus wind turbines and the signal-independent disturbance energies, respectively, at the output of the i-th filter associated to the k-th radar cell. Hence, to guarantee target detectability regardless of its actual velocity and location, the following figure of merit is assumed:

$$\mathrm{SINR}_B = \min_{k=1,\ldots K,\ i\in\mathcal{A}_k} \mathrm{SINR}_{k,i} \quad (13)$$

namely the worst-case SINR at the output of the filter array, corresponding to the minimum SINR among the available branches, each tuned to a specific velocity.

Both an energy and a similarity constraint are forced on the transmit sequence. The former rules the energy budget and is given by $\|\boldsymbol{s}\|^2 = 1$; the latter controls some critical properties of the probing signal [8] and is defined as:

$$\|\boldsymbol{s} - \boldsymbol{s}_0\|^2 \leq \tau \quad (14)$$

where the parameter $0 \leq \tau \leq 2$ rules the size of the trust hypervolume and $\boldsymbol{s}_0$ is a prefixed code. Based on above guidelines, the joint design of the radar code and the receive architecture can be formulated as the following constrained max-min optimization problem

$$\mathcal{P}\ \begin{cases} \max\limits_{\boldsymbol{s},\{\boldsymbol{w}_{k,i}\}} & f(\boldsymbol{s},\boldsymbol{w}_{1,1},\ldots,\boldsymbol{w}_{K,N_K}) \\ \text{s.t.} & \|\boldsymbol{s}\|^2 = 1 \\ & \|\boldsymbol{s}-\boldsymbol{s}_0\|^2 \leq \tau \end{cases} \quad (15)$$

where $N_k = |\mathcal{A}_k|$, $k = 1,\ldots,K$ and

$$f(\boldsymbol{s},\boldsymbol{w}_{1,1},\ldots,\boldsymbol{w}_{K,N_K}) = \min_{k=1,\ldots K,\ i\in\mathcal{A}_k} \mathrm{SINR}_{k,i} \quad (16)$$

Problem $\mathcal{P}$ is a non-convex optimization problem (the objective function is a non-convex function and $\|\boldsymbol{s}\|^2 = 1$ defines a non-convex set), and the solution techniques developed in [7], [9] cannot be used to handle it. It is thus necessary to develop a new optimization procedure to tackle this challenging problem. As first step toward this goal, following the same line of reasoning as in [7, Theorem 1], it can be shown that $\mathcal{P}$, for any $0 \leq \tau < 2$, is equivalent to:

$$\mathcal{P}_1\ \begin{cases} \max\limits_{\boldsymbol{s},\{\boldsymbol{w}_{k,i}\}} & f(\boldsymbol{s},\boldsymbol{w}_{1,1},\ldots,\boldsymbol{w}_{K,N_K}) \\ \text{s.t.} & \|\boldsymbol{s}\|^2 \leq 1 \\ & \Re\left(\boldsymbol{s}_0^\dagger\boldsymbol{s}\right) \geq \tau_1 \end{cases} \quad (18)$$

where $\tau_1 = 1 - \frac{\tau}{2} > 0$. Observe that $\mathcal{P}_1$ is still a non-convex optimization problem because the objective function is a non-convex function. Nonetheless, differently from $\mathcal{P}$, the equivalent formulation shares a convex feasible set. To handle $\mathcal{P}_1$ the optimization framework proposed in [10] is exploited, where two variable blocks are considered. One is the transmit signal, while the other is the set of all the receive filters. Hence, the following optimization problems have to be alternatively solved:

$$\mathcal{P}_{\boldsymbol{s}}{}^{(n)}\ \begin{cases} \max\limits_{\boldsymbol{s}} & f_1\left(\boldsymbol{s},\boldsymbol{w}_{1,1}^{(n-1)},\ldots,\boldsymbol{w}_{K,N_K}^{(n-1)}\right) \\ \text{s.t.} & \|\boldsymbol{s}\|^2 \leq 1 \\ & \Re\left(\boldsymbol{s}_0^\dagger\boldsymbol{s}\right) \geq \tau_1 \end{cases}$$

and

$$\mathcal{P}_{\boldsymbol{w}}{}^{(n)}\ \left\{\ \max_{\{\boldsymbol{w}_{k,i}\}}\ f\left(\boldsymbol{s}^{(n)},\boldsymbol{w}_{1,1},\ldots,\boldsymbol{w}_{K,N_K}\right)\right.$$

$$f_1\left(\boldsymbol{s}, \boldsymbol{w}_{1,1}, \ldots, \boldsymbol{w}_{K,N_K}\right) = \min_{k=1,\ldots K,\ i\in\mathcal{A}_k} \frac{-\mathrm{E}_{\boldsymbol{s}}^{(k,i)} + 2\Re\left\{\boldsymbol{y}_{\boldsymbol{s}}^{(k,i)}\boldsymbol{s}\right\}}{\boldsymbol{w}_{k,i}^{\dagger}\boldsymbol{\Sigma}_{\boldsymbol{d}}^{(k)}\left(\boldsymbol{s}\right)\boldsymbol{w}_{k,i} + \boldsymbol{w}_{k,i}^{\dagger}\boldsymbol{\Sigma}_{\boldsymbol{n}}\,\boldsymbol{w}_{k,i}} \tag{17}$$

where the function $f_1\left(\boldsymbol{s}, \boldsymbol{w}_{1,1}, \ldots, \boldsymbol{w}_{K,N_K}\right)$ is reported in (17) and:

$$\begin{aligned}
\mathrm{E}_{\boldsymbol{s}}^{(k,i)} &= \sum_{q=1}^{Q} \mathrm{var}\left(\alpha^{(q,k)}\right)\left|\left(\boldsymbol{s}\odot\boldsymbol{p}\left(\mu_i^{(q)}\right)\right)^{\dagger}\boldsymbol{w}_{k,i}^{(q)}\right|^2 \\
\boldsymbol{y}_{\boldsymbol{s}}^{(k,i)} &= \boldsymbol{s}^{\dagger}\left(\sum_{q=1}^{Q}\mathrm{var}\left(\alpha^{(q,k)}\right)\boldsymbol{A}_{k,i}^{(q)}\right) \\
\boldsymbol{A}_{k,i}^{(q)} &= \mathrm{diag}\left(\boldsymbol{p}\left(\mu_i^{(q)}\right)^{\dagger}\right)\boldsymbol{w}_{k,i}^{(q)}\boldsymbol{w}_{k,i}^{(q)}\mathrm{diag}\left(\boldsymbol{p}\left(\mu_i^{(q)}\right)\right)
\end{aligned}$$

Problems $\mathcal{P}_{\boldsymbol{s}}{}^{(n)}$ and $\mathcal{P}_{\boldsymbol{w}}{}^{(n)}$ are solvable. Hence, it can be shown that the devised algorithm monotonically converges to the limit value associated with the employed starting point ensuring the algorithm stability (in terms of convergence). As to $\mathcal{P}_{\boldsymbol{w}}{}^{(n)}$, a closed form optimal solution $\left(\boldsymbol{w}_{1,1}^{(n)}, \ldots, \boldsymbol{w}_{K,N_K}^{(n)}\right)$ for any fixed $\boldsymbol{s}^{(n)}$ can be obtained. For conciseness, the demonstrations of these is kept for an extended publication. However, it is worth mentioning that, for each velocity bin, the optimisation procedure fundamentally picks up the best receiver among the available ones, also lowering the computational complexity since there is no need of jointly process the signals coming from the Q receivers. As to the solution of Problem $\mathcal{P}_{\boldsymbol{s}}{}^{(n)}$ we exploit[5] some results from the Generalised Fractional Programming (GFP) theory [11], [12], which are summarized here in the form of a lemma.

Lemma 3.1: Let $\mathcal{X} \subseteq \mathbb{C}^N$ be a convex compact set, $\{f_i(\boldsymbol{x})\}_{i=1}^{I}$ be non-negative concave functions over $\mathcal{X}$, and $\{g_i(\boldsymbol{x})\}_{i=1}^{I}$ positive convex functions over $\mathcal{X}$. Hence, the GFP problem

$$P_{GFP}\left\{\begin{array}{ll}\max\limits_{\boldsymbol{x}} & \min\limits_{i=1,\ldots,I}\dfrac{f_i(\boldsymbol{x})}{g_i(\boldsymbol{x})} \\ \text{s.t.} & \boldsymbol{x}\in\mathcal{X}\end{array}\right. , \tag{19}$$

is solvable and an optimal solution can be obtained through **Algorithm 1**[6].

Algorithm 1 is characterized by a linear convergence rate [11] and, in each iteration, only requires the solution of a convex problem, which can be obtained in polynomial time using many convex programming algorithms [13]. Additionally, the objective function of P_{GFP} monotonically converges to the optimal value of P_{GFP} and the exit condition $F_\lambda = 0$, in practice, is replaced by $F_\lambda \leq \varsigma$, with ς a prescribed accuracy. ■

[5]Without loss of generality, some proper linear inequalities can be added to $\mathcal{P}_{\boldsymbol{s}}{}^{(n)}$.

[6]It is worth pointing out that the convergence of **Algorithm 1** to an optimal solution of P_{GFP} holds even under some milder technical conditions [11], [12].

Algorithm 1 : Generalized Dinkelbach's Algorithm

Input: $\mathcal{X}\subseteq\mathbb{C}^N$, $\{f_i(\boldsymbol{x})\}_{i=1}^{I}$, and $\{g_i(\boldsymbol{x})\}_{i=1}^{I}$.
Output: A solution $\boldsymbol{x}^\star$ to P_{GFP}.
1: set $n=0$, $\lambda_n=0$.
2: **do**
3: find $\boldsymbol{x}_n^\star = \arg\max\limits_{\boldsymbol{x}\in\mathcal{X}}\left\{\min\limits_{1\leq i\leq I} f_i(\boldsymbol{x}) - \lambda_n g_i(\boldsymbol{x})\right\}$;
4: let $F_\lambda = \left\{\min\limits_{1\leq i\leq I} f_i(\boldsymbol{x}_n^\star) - \lambda_n g_i(\boldsymbol{x}_n^\star)\right\}$;
5: $n = n+1$;
6: $\lambda_n = \min\limits_{1\leq i\leq I}\dfrac{f_i(\boldsymbol{x}_{n-1}^\star)}{g_i(\boldsymbol{x}_{n-1}^\star)}$;
7: **until** $F_\lambda = 0$
8: output $\boldsymbol{x}^\star = \boldsymbol{x}_{n-1}^\star$.

A. Transmit-Receive System Design: Optimization Procedure

In this subsection, the devised sequential optimization procedure is summarized as **Algorithm 2**. To trigger the recursion, an initial radar code $\boldsymbol{s}^{(0)}$ from which obtaining the optimal filter bank $\left(\boldsymbol{w}_{1,1}^{\star}{}^{(0)}, \ldots, \boldsymbol{w}_{K,N_K}^{\star}{}^{(0)}\right)$ is required; a natural choice is $\boldsymbol{s}^{(0)} = \boldsymbol{s}_0$.

Algorithm 2 : Algorithm for Transmit-Receive System Design

Input: $\mathrm{var}\left(\alpha^{(q,k)}\right)$, $\mathrm{var}\left(\beta_{m,l}^{(q,k)}\right)$, $\mathrm{var}\left(\gamma_{k'}^{(q,k)}\right)$, $\overline{\nu}_{m,l}^{(q,k)}, \delta_{m,l}^{(q,k)}, \overline{\xi}_{k'}^{(q,k)}, \varepsilon_{k'}^{(q,k)}$, $\boldsymbol{\Sigma_n}$, $\mu_i^{(q)}$, $\boldsymbol{s}_0$, τ.
Output: A solution $\left(\boldsymbol{s}^\star, \boldsymbol{w}_{1,1}^\star, \ldots, \boldsymbol{w}_{K,N_K}^\star\right)$ to $\mathcal{P}$.
1: set $n=0$ and $\boldsymbol{s}^{(n)} = \boldsymbol{s}_0$, and compute $\boldsymbol{w}_{k,i}^{\star}{}^{(n)}$ for $k=1,\ldots,K$, $i=1,\ldots,N_K$ through the closed-form solution of problem $\mathcal{P}_{\boldsymbol{w}}{}^{(n)}$, and $\mathrm{SINR}^{(n)} = f\left(\boldsymbol{s}^{(n)}, \boldsymbol{w}_{1,1}^{\star}{}^{(n)}, \ldots, \boldsymbol{w}_{K,N_K}^{\star}{}^{(n)}\right)$;
2: **do**
3: $n = n+1$;
4: solve problem $\mathcal{P}_{\boldsymbol{s}}{}^{(n)}$ finding an optimal radar code $\boldsymbol{s}^{\star(n)}$, through the use of **Algorithm 1**;
5: solve problem $\mathcal{P}_{\boldsymbol{w}}{}^{(n)}$ finding an optimal receive filter bank $\boldsymbol{w}_{k,i}^{\star}{}^{(n)}$.
6: let $\mathrm{SINR}^{(n)} = f\left(\boldsymbol{s}^{\star(n)}, \boldsymbol{w}_{1,1}^{\star}{}^{(n)}, \ldots, \boldsymbol{w}_{K,N_K}^{\star}{}^{(n)}\right)$;
7: **until** $|\mathrm{SINR}^{(n)} - \mathrm{SINR}^{(n-1)}| \leq \zeta$
8: output $\boldsymbol{s}^\star = \boldsymbol{s}^{\star(n)}$ and $\boldsymbol{w}_{k,i}^\star = \boldsymbol{w}_{k,i}^{\star}{}^{(n)}$, $k=1,\ldots,K$, $i=1,\ldots,N_k$.

IV. Performance Analysis

In order to assess the performance of the proposed framework, a simple scenario is simulated and analysed. The surveil-

lance area is divided into 10×10 cells whose dimension is $100\,\mathrm{m} \times 100\,\mathrm{m}$, numbered from 1 to 100 along the rows from the bottom-left corner (thus cell 1 coincides with the origin of the reference system). Two sensors are located in cells 1 and 10, respectively, with the first one being transmitter/receiver, while two wind turbines are located in 5 and 76. The first one has a rotation speed of 0.24 Rounds per Second (RPS) and faces south, while the second turbine turns at 0.20 RPS and faces south-east. Furthermore, the turbines have $L = 3$ blades of 45 m each, discretised as $M = 10$ points scatterers, with $\mathrm{var}\left(\beta_{m,l}^{(q,k)}\right) = 10/(L \times M)$. Regarding the radar, it transmits a sequence of $N = 20$ phase coded pulses in L-band with $PRI = 1/2\,\mathrm{ms}$. The reference code $\boldsymbol{s}_0$ for the similarity constraint is a generalised Barker code, a constant modulus sequence exhibiting good correlation properties. Finally, the number of filters per receiver is 20.

A uniformly distributed clutter is assumed over the normalised Doppler interval $\left[\overline{\xi}_{k'}^{(q,k)} - \varepsilon_{k'}^{(q,k)}, \overline{\xi}_{k'}^{(q,k)} + \varepsilon_{k'}^{(q,k)}\right] = [-0.065, 0.065]$, with $\mathrm{var}\left(\gamma_{k'}^{(q,k)}\right) = 1000/\left(N_C + 1\right)$ and $N_C = 1$. As to the signal-independent disturbance, it is assumed $\boldsymbol{\Gamma}_{\boldsymbol{n}}^{(q)} = \boldsymbol{I}$. Finally, $\mathrm{var}\left(\alpha^{(q,k)}\right) = 10$.

The convex optimization problems are solved via the CVX toolbox. The exit condition in **Algorithm 2** assumes $\zeta = 10^{-3}$, whereas that in **Algorithm 1** $\varsigma = 10^{-6}$.

In figure 1 the results of the simulation for two different values of the similarity constraint τ are shown. In both the cases, the optimisation procedure leads to an improvement of the worst-case SINR, $SINR_B$, of about $3.6\,d$B. As expected, $SINR_B$ is slightly lower when the similarity constraint τ is tighter, but also the convergence of the algorithm is faster. In particular, for the case in which $\tau = 0.2$ the maximum $SINR_B$ is 9.28 dB in 113 iterations while when $\tau = 0.5$ the maximum $SINR_B$ is 9.36 dB in 139 iterations.

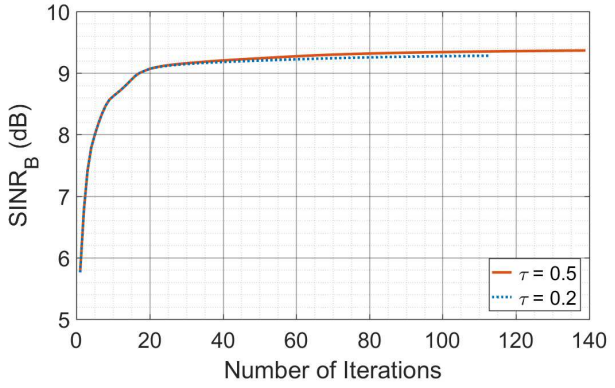

Fig. 1: Analysis results: $SINR_B$ monotonically increasing property of the proposed method.

V. Conclusion

This paper proposed a joint radar waveform and filter design aimed to optimize the SINR in a multi-static radar scenario in the presence of wind turbine interference. The proposed framework allows to jointly adjust the slow-time radar waveform and the weights of the receiver filters. In particular an iterative algorithm that monotonically improves the worst case system SINR is developed. The computational complexity of the proposed method is linear with the number of outer iterations whereas at each iteration, it mainly requires the implementation effort of the Dinkelbach's procedure. The performance assessed on simulated data showed that the proposed method is effective in rejecting the interference from the wind farms, with an improvement of the worst-case SINR of more than $4\,d$B.

References

[1] F. Kong, Y. Zhang, and R. D. Palmer, "Wind turbine radar interference studies by polarimetric measurements of a scaled model," *IEEE Transactions on Aerospace and Electronic Systems*, vol. 49, no. 3, pp. 1589–1600, July 2013.

[2] C. Clemente and J. J. Soraghan, "Analysis of the effect of wind turbines in sar images," in *IET International Conference on Radar Systems (Radar 2012)*, Oct 2012, pp. 1–4.

[3] F. Fioranelli, M. Ritchie, A. Balleri, and H. Griffiths, "Practical investigation of multiband mono- and bistatic radar signatures of wind turbines," *IET Radar, Sonar Navigation*, vol. 11, no. 6, pp. 909–921, 2017.

[4] S. I. Krich, M. Montanari, V. Amendolare, and P. Berestesky, "Wind turbine interference mitigation using a waveform diversity radar," *IEEE Transactions on Aerospace and Electronic Systems*, vol. 53, no. 2, pp. 805–815, April 2017.

[5] R. M. Beauchamp and V. Chandrasekar, "Suppressing wind turbine signatures in weather radar observations," *IEEE Transactions on Geoscience and Remote Sensing*, vol. 55, no. 5, pp. 2546–2562, May 2017.

[6] W. He, Q. Zhai, X. Wang, and R. Wu, "Mitigation of wind turbine clutter based on the periodicity in scanning atc radar," in *IET International Radar Conference 2015*, Oct 2015, pp. 1–6.

[7] A. Aubry, A. D. Maio, and M. M. Naghsh, "Optimizing Radar Waveform and Doppler Filter Bank via Generalized Fractional Programming," *IEEE Journal of Selected Topics in Signal Processing*, vol. 9, no. 8, pp. 1387–1399, Dec 2015.

[8] J. Li, J. R. Guerci, and L. Xu, "Signal Waveform's Optimal-Under-Restriction Design for Active Sensing," *IEEE Signal Processing Letters*, vol. 13, no. 9, pp. 565–568, Sept 2006.

[9] A. Aubry, A. DeMaio, A. Farina, and M. Wicks, "Knowledge-Aided (Potentially Cognitive) Transmit Signal and Receive Filter Design in Signal-Dependent Clutter," *IEEE Transactions on Aerospace and Electronic Systems*, vol. 49, no. 1, pp. 93–117, Jan 2013.

[10] M. Razaviyayn, M. Hong, and Z.-Q. Luo, "A Unified Convergence Analysis of Block Successive Minimization Methods for Nonsmooth Optimization," *SIAM Journal on Optimization*, vol. 23, no. 2, pp. 1126–1153, 2013.

[11] J.-P. Crouzeix and J. A. Ferland, "Algorithms for generalized fractional programming," *Mathematical Programming*, vol. 52, no. 1, pp. 191–207, May 1991.

[12] A. I. Barros, J. B. G. Frenk, S. Schaible, and S. Zhang, "A new algorithm for generalized fractional programs," *Mathematical Programming*, vol. 72, no. 2, pp. 147–175, Feb 1996.

[13] M. Grant and S. Boyd. (2012, February) CVX package. [Online]. Available: http://www.cvxr.com/cvx